Effect of nuclear corrections on the parton distribution functions of a bound nucleon and EMC ratio of $A = 3$ nuclei in a dressed-quark scenario

Mohammad Rasti*

Physics Department, Faculty of Science, Razi University, 67149-67346 Kermanshah, Iran

(Received 24 October 2018; published 4 April 2019)

By using the valence quark exchange model, the up- and down-quark distribution functions as the distributions of three constituent quark inside the bound nucleons have been extracted and will be used in the context of the Altarelli, Cabibbo, Maiani, and Petronzio (ACMP) constituent quark model formalism to calculate the different pointlike parton distribution functions of the bound nucleons and the structure functions of ^{3}He and ^{3}H mirror nuclei at the energy scale of $Q^2 = 4$ GeV^2. In the latter picture the constituent quarks are assumed to be complex objects, made of pointlike partons which can be pointlike valence quarks, pointlike sea quarks, and pointlike neutral gluons. The sea quark and the gluon contributions to the structure functions of the helium-3 and the tritium nuclei have been analyzed in this scale of energy by reparameterizing the ACMP constituent quark model formalism. Unlike our previous works, where the parton densities inside the nucleon have been computed at the hadronic scale of energy, i.e., $Q_0^2 = 0.34$ GeV^2, and then those distributions have been evolved to the high-energy scales by using the Dokshitzer, Gribove, Lipatov, Altarelli, and Parisi evolution equations, in the present study the parton distribution functions have been calculated at the energy scale of $Q^2 = 4$ GeV^2 directly by using the new parameters in the context of the dressed-quark scenario. Thus, at the first step, the extracted partonic distributions have been considered to calculate the nucleons and the nuclei structure functions and then the ratios of the neutron to the proton and ^{3}He to ^{3}H nuclei structure functions as well as the European Muon Collaboration ratios for the valence quark distributions, ^{3}He and ^{3}H nuclei, are calculated. The results are in a good agreement with both theoretical and available experimental data.

DOI: 10.1103/PhysRevC.99.044302

I. INTRODUCTION

Several electron deep inelastic scattering (DIS) experiments have been carried out on the various polarized and unpolarized nucleon and nucleus targets, for instance, the proton, deuterium, helium-3, tritium, etc., to attain some knowledge about the partonic structure of hadrons and nuclei like valence-up and -down quarks, sea quark-antiquarks, and neutral gluons [1–7].

In order to investigate and explain the results of these experiments, various theoretical models and interpretations have been suggested [8,9]. One of these theoretical models is the valence quark exchange model (QEM), that originally was presented in 1987 to explain the deviation from unity of the ratios of the structure functions of the bound nucleon to that of the free nucleon [10,11]. This ratio, called the EMC ratio, the name that was adopted after the discovery of the European Muon Collaboration group, Aubert *et al.* [1], has been investigated by both theoretical and experimental groups [12–23].

The polarized and unpolarized QEM have been used in several theoretical research works to study the structured content of the nuclei. The results of these calculations show a reasonable agreement with the outcomes of the corresponding experiments [11,18–27]. In this formalism, it is assumed that the exchange of the valence constituent quarks between the nucleons bound in the nucleus could be considered to explain the partonic structure of the nuclei; moreover, such an exchange may have a noticeable contributions or perhaps domain to the EMC ratio [10]. Also, this model has been successfully used in the context of the chiral quark model to investigate both the transverse momentum dependence of the parton distribution functions [28] and the EMC ratio of the helium-3 and tritium nuclei [29]. Recently, the QEM framework was successfully used in the very small-x region to calculate the unintegrated parton distribution functions (UPDF) of the ^{6}Li structure function with six nucleons, in which the results show an extreme improvement in the calculation of the partonic distribution functions of the bound nucleons and also the predictions have an excellent agreement with the NMC experimental data [30]. It should be mentioned that the study of the UPDF in the case of the nuclei were proposed by de Oliveira *et al.* [31] and they have shown that the structure function of the nucleus can get a very good modification in the very small-x region by considering the UPDF.

Another point worth noting is by considering the sea quark-antiquark pairs and gluons as the new degrees of freedom in the framework of QEM, the calculations of the model became dramatically very complicated but, due to the important role of the sea quark and the gluon at the small-x regions [32–34], it was very important to include them to shed some light on to this x region in the context of QEM.

*m.rasti@razi.ac.ir, mohammad.rasti@gmail.com

To study the above degrees of freedom and to estimate their contributions to the QEM, the Altarelli, Cabibbo, Maiani, and Petronzio (ACMP) constituent quark model formalism have been used. In fact, this scheme was proposed by them in the background of SU(2) × O(3) to investigate the nucleon structure function from the idea that the constituent quarks themselves have a structure [35]. It should be noted that the ACMP constituent quark model is not the only constituent quark model and other model schemes such as the chiral quark model [36–40], the valon model [41,42], and the bag model [43] have been also suggested.

In the framework of the constituent quark model (CQM), each constituent quark is assumed to be a complex object dressing the valence pointlike (PL) quark with the PL quark-antiquark pairs and the PL neutral gluons as its constituents in quantum chromodynamics (QCD). The compatibility of this suggestion with QCD have been checked; moreover, it is shown that the constituent quark that is made by the dressed QCD Lagrangian field is consistent with the concept of the color confinement [44].

The CQM has been used in different studies with various contexts to calculate the structured content of the unpolarized nucleon [45–53], the structure function of polarized nucleons [54], and the pion structure function [55]. Recently, this formalism has been used to extract the bound parton distribution function in proton [56], helium-3, and tritium [57] and the $A = 6$ isoscalar system [58]. The results of all these works have been reasonably in good agreement with the corresponding experimental data. It should be mentioned that it would be possible to calculate the generalized parton distribution functions (GPDs) and transverse momentum dependence (TMDs) in the context of the ACMP constituent quark exchange model. This issue could proceed because the present model could be extended [21,28,59] to calculate the GPD and TMD as we hope to study this subject in the future works to compare the results with the outcome of the Jefferson Laboratory (JLab) data and although some investigations that have been done [60–62].

Thus, the purpose of this paper at the first step is to use the quark exchange model in the framework of the constituent quark model formalism to extract the various bound parton distributions like PL valence-up and -down quarks, PL sea quarks, and PL gluon distributions. Furthermore, by using these distributions, the structure functions of the bound and the free nucleon and also the nuclear structure-function targets have been calculated. Then, the EMC ratios of the valence quarks, ^{3}He and ^{3}H nuclei, are extracted. Finally, the ratio of the helium-3–to-tritium structure functions as well as the ratio of the neutron-to-proton structure functions have been derived.

The paper will be organized as follows: In Sec. II, the ACMP constituent quark model formalism is introduced and the parameters of the model at the new scale of energy i.e., $Q_0^2 = 4$ GeV^2, have been shown. The procedure of extracting the $\mathcal{U}$-type and $\mathcal{D}$-type constituent quark distribution functions in the bound nucleons as the input for the CQM are obtained by using the QEM for three-nucleon systems such as helium-3 and tritium nuclei which have been discussed in Appendix. In Sec. III, the next-to-leading-order (NLO) level of the nucleus structure functions in terms of the PL parton distribution functions as well as the procedure of calculating the structure functions of the free nucleon have been clearly defined. Our results and discussions related to the different PL partons distributions, the structure function of ^{3}He and ^{3}H nuclei, their EMC ratios, and the ratio of the neutron-to-proton structure functions are discussed in Sec. IV. Finally, in Sec. V, our conclusion will be given.

II. PARTON DENSITIES IN ACMP CONSTITUENT QUARK MODEL

In this section, I start with a brief summary of the constituent quark model formalism. In this model the constituent quark (CQ) is assumed to be a complex object and their weak and electromagnetic structure functions are defined in terms of the functions $\Phi_{q/\mathrm{CQ}}(x)$ that specify the number of PL partons type q inside the $\mathcal{U}$-type or $\mathcal{D}$-type constituent quark, with a fraction x of its total momentum. These functions are not all independent, but they are restricted by isospin and charge conjugation [35]. The $\Phi_{q/\mathrm{CQ}}(x)$ are called the structure functions of the constituent quarks [35,46]. As a consequence, the parton distributions in a nucleon can be expressed, according to the structure function of the constituent quarks and the probability distributions of the up- and down-constituent quarks inside the nucleon, i.e., $G_{\mathcal{U}/N}$ and $G_{\mathcal{D}/N}$, as follows:

$$xq(x,Q_0^2) = \int_x^1 x\frac{dy}{y}\left[\Phi_{q/\mathcal{U}}\left(\frac{x}{y},Q_0^2\right)G_{\mathcal{U}/N}(y,Q_0^2) + \Phi_{q/\mathcal{D}}\left(\frac{x}{y},Q_0^2\right)G_{\mathcal{D}/N}(y,Q_0^2)\right]. \quad (1)$$

In this equation, labels q represents the different PL partons such as the PL valence quarks, u_{val} and d_{val}, the PL sea quarks, q_{sea}, and the PL gluons, g, where the Q_0^2 is the momentum scale, at which the parameters of the CQM will be defined. Also in Eq. (1) $G_{\mathcal{U}/N}(y,Q_0^2)$ and $G_{\mathcal{D}/N}(y,Q_0^2)$ are the probability distribution functions of the $\mathcal{U}$-type and $\mathcal{D}$-type constituent quarks, respectively, having momentum fraction y of the bound nucleon at Q_0^2.

The functional forms of the constituent quark structure functions of the various types, would be extracted by taking three natural assumptions, namely the determination of the PL partons by the QCD, the Regge behavior for $x \to 0$ and the duality idea [35,55], and, finally, the isospin and the charge conjugate invariant. By taking these considerations into account, for different kind of the parton structure functions inside the constituent quark, the following definition have been proposed [46]:

$$\Phi_{\mathrm{q/CQ}}(x) = \alpha_q\, x^{\beta_q}(1-x)^{\eta_q-1}, \quad (2)$$

where $q = q_{\mathrm{val}}$, q_{sea}, g denote valence quarks, sea quarks, and the gluons, respectively. As it was shown in Refs. [35,48], the value of $\beta_{q_{\mathrm{val}}}$ have been derived -0.5 that was concluded in order to describe the Regge behavior, i.e., the ρ meson exchanged and $\beta_{q_{\mathrm{sea}}} = \beta_g = -1$ from pomeron exchange. By considering these points, the various pointlike parton distributions inside the constituent quarks will be given by the following relations:

(i) for the case of valence quark distributions in CQ,

$$\Phi_{q_{\rm val}/{\rm CQ}}\left(x, Q_0^2\right) = \alpha_{q_{\rm val}}\, x^{-0.5}(1-x)^{\eta_{q_{\rm val}}-1}, \tag{3}$$

(ii) for the sea quarks in CQ, related structure function is

$$\Phi_{q_{\rm sea}/{\rm CQ}}\left(x, Q_0^2\right) = \alpha_{q_{\rm sea}}\, x^{-1}(1-x)^{\eta_{q_{\rm sea}}-1}, \tag{4}$$

and, finally, (iii) the probability distribution of the gluons in CQ is as follows:

$$\Phi_{g/{\rm CQ}}\left(x, Q_0^2\right) = \alpha_g\, x^{-1}(1-x)^{\eta_g-1}. \tag{5}$$

Note that the QCD sum rules indicate that each constituent quark contains only one valence quark; therefore, Eq. (3) should satisfy the following relation at all values of Q^2:

$$\int_0^1 \Phi_{q_{\rm val}/{\rm CQ}}\left(x, Q_0^2\right)dx = 1. \tag{6}$$

By substituting Eq. (3) in this renormalization condition, the parameter $\alpha_{q_{\rm val}}$ will be determined as follows:

$$\alpha_{q_{\rm val}} = \frac{\Gamma\left(\eta_{q_{\rm val}} + \frac{1}{2}\right)}{\Gamma(\eta_{q_{\rm val}})\Gamma\left(\frac{1}{2}\right)}. \tag{7}$$

where it should be mentioned that the numerical values of $\eta_{q_{\rm val}}$ will be listed later. The other parameters of the model can be extracted by using the approach of Ref. [35]. We choose the $Q_0^2 = 4$ GeV^2, because the momentum that has been carried by different partons are well known experimentally at this Q_0^2. We use the data of Ref. [63] to calculate the second moments of the different partons. By using these data, it has been derived that 28.65% of the nucleon momentum is carried by the valence-up quarks, 10.34% by the valence-down quarks, 45.60% by the gluons, and the remaining momentum are belong to the sea quarks. Thus, by using the derived second moments of the various parton distribution functions, the parameters $\eta_{q_{\rm val}}$, η_g, α_g and the ratio $\alpha_{q_{\rm sea}}/\eta_{q_{\rm sea}}$ at $Q_0^2 = 4$ GeV^2 scale of energy will be determined. As discussed in Refs. [35,46], the remaining parameter, $\alpha_{q_{\rm sea}}$ (or $\eta_{q_{\rm sea}}$), which describes the sea-quark distributions, has been evaluated through the value of the unpolarized structure function $F_2^{\rm ep}$ at low x, where the sea quarks in these regions are known to be dominant. The value of $F_2^{\rm ep}$ at $x = 10^{-2}$ for this scale of energy has been used, as given by the fit of GRV [63], which are in a good agreement with available data. So, in this scale, the parameters of the model take the following values:

$$\alpha_{q_{\rm sea}} = 0.075; \alpha_g = 0.439, \tag{8}$$

$$\eta_{q_{\rm val}} = 0.65; \eta_{q_{\rm sea}} = 2.918; \eta_g = 0.2, \tag{9}$$

It should be mentioned that the ACMP constituent quark model formalism also have been used to extract the partonic content of the pion structure [55], in which the parameters have been obtained at the same Q^2 but with a different number of active flavors, N_f, and different QCD cut-off, Λ. In fact at sufficiently low Q^2, the effective QCD coupling, $\alpha_s(Q^2)$, will become large. It is common to show that Q^2 scale at which this happens by Λ^2. It is natural to take the Λ^2 as marking the boundary between a world of quasifree quarks and gluons and the world of strongly coupled world of pions, protons, and so on. It is expected that the value of Λ would be of the order of a typical hadronic mass.

In Eq. (3) the CQ (q_v) can be equal to $\mathcal{U}$ ($u_{\rm val}$) or $\mathcal{D}$ ($d_{\rm val}$), which are the $\mathcal{U}$-type constituent quark (PL valence-up quark) and $\mathcal{D}$-type constituent quark (PL valence-down quark). One should noted that $\Phi_{d_{\rm val}/\mathcal{U}}(x, Q_0^2)$ and $\Phi_{u_{\rm val}/\mathcal{D}}(x, Q_0^2)$ are zero, because in the $\mathcal{U}$-type CQ, there is no net quark valence type d and vice versa. Besides this, as will be shown in the next section, $G_{\mathcal{U}/N}(y, Q_0^2)$ and $G_{\mathcal{D}/N}(y, Q_0^2)$ have a different functional form in the valence QEM; therefore, the different form for $u_{\rm val}(x, Q_0^2)$ and $d_{\rm val}(x, Q_0^2)$ will be obtained from Eq. (1), but for the sea quarks or the gluons in the nucleon bound in the nucleus the same distributions will be extracted because in the case of the PL sea quarks $[q_{\rm sea}(x, Q_0^2)]$ and the PL gluons $[g(x, Q_0^2)]$, there is no flavor dependent as it is presented in Eqs. (4) and (5).

In fact, in the ACMP constituent quark model formalism, it is assumed that the gluons will produce equally all the sea quark flavors, e.g., u-$\bar{u}$ pair generated as the same as the pair of d-$\bar{d}$, therefore; there is no flavor dependence of the PL gluons. As a consequence, in this work it is not possible to analyze the effects of the flavor dependence of the sea quarks as well as the flavor dependence of the gluons hence the SU(2) symmetry breaking of the nucleon sea in the context of the CQM cannot be checked, the fact imposed by the observed Gottfried sum rule [64,65]. We hope to study this issue in our next works in the framework of the CQM.

III. STRUCTURE FUNCTIONS OF $A = 3$ NUCLEI AND EMC RATIO

In the preceding section, I will discuss the calculation of the structure functions of the light nuclei by taking the momentum density distribution for the constituent quarks in the nuclear environment. By the rule and the definition of the structure function, it measures the distribution of the quarks as a function of k^+/P^+ (the ratio of the light-cone momentum of the initial quark to the momentum of the proton) in the target rest frame which is equivalent to boost the nucleus to an infinite-momentum frame. This is usually done in the literature by using an *ad hoc* prescription for k^0 as a function of $|\vec{k}|$ as follows:

$$k^0 = [(\vec{k}^2 + m^2)^{\frac{1}{2}} - \epsilon_0]. \tag{10}$$

The sensitivity analysis of this hypothesis is verified and it is shown that the calculating structure functions are not sensitive to this assumption [10,11,66]. So, the constituent quark distributions at each $Q^2 = Q_0^2$, can be related to the momentum density distributions for each flavor in the nucleon of the nucleus A_i, according to the following equation [$j = p$, n ($a = \mathcal{U}, \mathcal{D}$) for proton (up constituent quark) and neutron (down constituent quark), respectively]:

$$q_j^{\,a}\left(y, Q_0^2; A_i\right) = \frac{1}{(1-y)^2}\int \rho_j^a(\vec{k}; A_i)\delta\left[\frac{y}{(1-y)} - \frac{k_+}{M_t}\right]d\vec{k}. \tag{11}$$

After doing the angular integration, we get

$$q_j^{\,a}\left(y, \mu_0^2; A_i\right) = \frac{2\pi M_t}{(1-y)^2}\int_{k_{\rm min}^a}^{\infty} \rho_j^a(\vec{k}; A_i)k\, dk, \tag{12}$$

with

$$k^a_{\min}(y) = \frac{1}{2}\left(\frac{yM_t}{1-y} + \epsilon^a_0\right) - \frac{m_a^2}{2}\frac{1}{\left(\frac{yM_t}{1-y} + \epsilon^a_0\right)}. \quad (13)$$

Equations (12) and (13) have been calculated by considering the relativistic and the covariant properties [67]. In these equations, M_t and m_a denote the nucleon up and down quark masses, respectively. The binding energy of quarks inside the bound nucleons are given by ϵ^a_0. It should be mentioned that, according to Refs. [10,11,19,20] and our Gaussian choice for the nucleon wave function in terms of quarks, see Appendix, the above issue is not working properly near $x = 1$, because the structure-function probe quark is very far from their mass shell. Also, the present prescription is different from those works, e.g., Ref. [68], in which only the nuclear effects are regarded. It should be mentioned that Eq. (11) is not covariant but this procedure is dynamically justified. In fact, it assumed that the final-state interaction effects could produce a PDF of the form of the Eq. (11) which has correct support. This fundamental feature can be analytically reached without any assumptions on the dynamics by using the relativistic Light-Front approach, especially for the case of the nuclear target, which has been described in more detail in Ref. [69].

By using the averaged mass for the proton and the neutron, i.e., $M_t = M_{\mathcal{N}} = \frac{1}{2}(M_p + M_n)$ in Eq. (12), the $\mathcal{U}$-type and $\mathcal{D}$-type constituent quark distributions in the helium-3 and the tritium targets are obtained in the following form, respectively [57]:

$$G_{\mathcal{U}/N}(y, Q_0^2; A_i) = \frac{2\pi M_{\mathcal{N}}}{(1-y)^2}\int_{k^u_{\min}}^{\infty} \rho_{\mathcal{U}}(k) k\, dk, \quad (14)$$

$$G_{\mathcal{D}/N}(y, Q_0^2; A_i) = \frac{2\pi M_{\mathcal{N}}}{(1-y)^2}\int_{k^d_{\min}}^{\infty} \rho_{\mathcal{D}}(k) k\, dk, \quad (15)$$

where A_i denotes the nucleus in which the constituent quark distributions have been calculated. Now, in order to calculate the different PL parton distributions inside the bound nucleons, i.e., $q = u_{\rm val},\ d_{\rm val},\ q_{\rm sea}$, and g, it is necessary to substitute the structure function of the constituent quark, $\Phi_{q/\rm CQ}(x)$, Eqs. (3)–(5), in addition to the $\mathcal{U}$-type and $\mathcal{D}$-type constituent quark distributions, $G_{\mathcal{CQ}/N}(y, Q_0^2; A_i)$, Eqs. (14) and (15), in the convolution integral relation of Eq. (1).

These discussions for the case of the PL up- and down-valence quarks, $u_{\rm val}(x, Q_0^2)$ and $d_{\rm val}(x, Q_0^2)$, take the following form:

$$xu_{\rm val}(x, Q_0^2) = \int_x^1 x\frac{dy}{y}\, G_{\mathcal{U}/N}(y, Q_0^2)\, \Phi_{u_{\rm val}/\mathcal{U}}\left(\frac{x}{y}, Q_0^2\right), \quad (16)$$

$$xd_{\rm val}(x, Q_0^2) = \int_x^1 x\frac{dy}{y}\, G_{\mathcal{D}/N}(y, Q_0^2)\, \Phi_{d_{\rm val}/\mathcal{D}}\left(\frac{x}{y}, Q_0^2\right), \quad (17)$$

The PL valence quark is the valence quark which will be calculated from the ACMP constituent quark model formalism, $u_{\rm val}$ and $d_{\rm val}$ from Eqs. (16) and (17), respectively. In fact, the PL valence quark distribution has been chosen to be different from those of the constituent quarks, $G_{\mathcal{U}/N}$ and $G_{\mathcal{D}/N}$. Also, the PL valence quark extracted from the combination of the $u_{\rm val} = u - \bar{u}$ and $d_{\rm val} = d - \bar{d}$ for the up- and down-quarks, respectively.

For the PL sea-quark distribution, $q_{\rm sea}(x, Q_0^2)$, and the PL gluon distribution, $g(x, Q_0^2)$, we get, respectively:

$$xq_{\rm sea}(x, Q_0^2) = \int_x^1 x\frac{dy}{y}\left[\Phi_{q_{\rm sea}/\mathcal{U}}\left(\frac{x}{y}, Q_0^2\right) G_{\mathcal{U}/N}(y, Q_0^2) + \Phi_{q_{\rm sea}/\mathcal{D}}\left(\frac{x}{y}, Q_0^2\right) G_{\mathcal{D}/N}(y, Q_0^2)\right], \quad (18)$$

$$xg(x, Q_0^2) = \int_x^1 x\frac{dy}{y}\left[\Phi_{g/\mathcal{U}}\left(\frac{x}{y}, Q_0^2\right) G_{\mathcal{U}/N}(y, Q_0^2) + \Phi_{g/\mathcal{D}}\left(\frac{x}{y}, Q_0^2\right) G_{\mathcal{D}/N}(y, Q_0^2)\right]. \quad (19)$$

Finally, the target structure function $\mathcal{F}_2^{A_i}(x, Q^2)$ in the NLO level is related to the various types of PL parton distribution functions like the valence-up and -down quarks, the sea quark, and the gluon distributions as follows [57,63]:

$$\mathcal{F}_2^{A_i}(x, Q^2) = x\sum_{\substack{a=u,d,s\\ [j=p,n]}} Q_a^2\left\{\left[q_j{}^a(x, Q^2; A_i) + \bar{q}_j{}^a(x, Q^2; A_i)\right] + \frac{\alpha_s(Q^2)}{2\pi}\left[q_j{}^a(x, Q^2; A_i) + \bar{q}_j{}^a(x, Q^2; A_i) + 2g_j^a(x, Q^2; A_i)\right]\right\}, \quad (20)$$

where the NLO coupling constant, $\alpha_s(Q^2)$, is as follows:

$$\frac{\alpha_s(Q^2)}{4\pi} \cong \frac{1}{\beta_0 \ln\left(\frac{Q^2}{\Lambda^2}\right)} - \frac{\beta_1 \ln\ln\left(\frac{Q^2}{\Lambda^2}\right)}{\beta_0^3 \ln(\frac{Q^2}{\Lambda^2})}, \quad (21)$$

in which β_0 and β_1 are the first two universal coefficients of the QCD β functions [63].

Thus, by taking these considerations into account and using the SU(6) symmetry, i.e.,

$$u^p_{\rm val}(x, Q^2) = d^n_{\rm val}(x, Q^2) = u_{\rm val}(x, Q^2),$$
$$d^p_{\rm val}(x, Q^2) = u^n_{\rm val}(x, Q^2) = d_{\rm val}(x, Q^2),$$
$$q_{\rm sea}(x, Q^2) = u_s(x, Q^2) = \bar{u}_s(x, Q^2) = d_s(x, Q^2) = \bar{d}_s(x, Q^2) = s_s(x, Q^2) = \bar{s}_s(x, Q^2),$$

the NLO level of the structure functions of helium-3 and tritium take the following forms, respectively:

$$\mathcal{F}_2^{^3\rm He}(x, Q^2) = x\left\{\frac{9}{4}\left(\frac{2}{3}\right)^2 u_{\rm val}(x, Q^2) + 6\left(\frac{1}{3}\right)^2 d_{\rm val}(x, Q^2) + 4q_{\rm sea}(x, Q^2) + \frac{\alpha_s(Q^2)}{2\pi}\left[u_{\rm val}(x, Q^2) + \frac{2}{3}d_{\rm val}(x, Q^2) + 4q_{\rm sea}(x, Q^2) + 4g(x, Q^2)\right]\right\}, \quad (22)$$

$$\mathcal{F}_2^{^3\mathrm{H}}(x,Q^2) = x\Big\{\frac{3}{2}\Big(\frac{2}{3}\Big)^2 u_{\mathrm{val}}(x,Q^2) + 9\Big(\frac{1}{3}\Big)^2 d_{\mathrm{val}}(x,Q^2) + 4q_{\mathrm{sea}}(x,Q^2) + \frac{\alpha_s(Q^2)}{2\pi}\Big[\frac{2}{3}u_{\mathrm{val}}(x,Q^2) + d_{\mathrm{val}}(x,Q^2) + 4q_{\mathrm{sea}}(x,Q^2) + 4g(x,Q^2)\Big]\Big\}. \tag{23}$$

So we have found the relation between the various PL parton distribution functions and ^{3}He and ^{3}H structure functions. Consequently, the EMC-type ratios for the structure functions of helium-3 and tritium can be obtained from the following definitions:

$$\mathcal{R}_{\mathrm{EMC}}^{^3\mathrm{He}}(x,Q^2) = \frac{\mathcal{F}_2^{^3\mathrm{He}}(x,Q^2)}{2\mathcal{F}_2^p(x,Q^2)+\mathcal{F}_2^n(x,Q^2)}, \tag{24}$$

$$\mathcal{R}_{\mathrm{EMC}}^{^3\mathrm{H}}(x,Q^2) = \frac{\mathcal{F}_2^{^3\mathrm{H}}(x,Q^2)}{\mathcal{F}_2^p(x,Q^2)+2\mathcal{F}_2^n(x,Q^2)}. \tag{25}$$

It should be noted that in Eqs. (24) and (25), the structure function of the proton and the neutron in the denominator are those of free nucleons.

Now the question raised is how to calculate the free-nucleon structure functions in the context of the constituent quark exchange model. In QEM the constituent up- and down-quark distribution functions inside the three-nucleon systems are related to their momentum density distributions, Eqs. (A10) and (A11), where in those equations $\mathcal{I}$ is the exchange integral due to the contribution of the nucleus wave function, $\chi(x,y,\cos\theta)$, to the constituent quark momentum distributions that have been derived as follows [11]:

$$\mathcal{I} = 8\pi^2 \int_0^\infty x^2\,dx \int_0^\infty y^2\,dy \int_{-1}^1 d(\cos\theta)\exp\Big[-\frac{3x^2}{4b^2}\Big] \times |\chi(x,y,\cos\theta)|^2. \tag{26}$$

So the answer to the above question is that by taking $\mathcal{I}=0$ in the constituent quark momentum distributions, one can get the parton densities inside the free nucleon, Eqs. (A10) and (A11), where it means that the nucleons are sufficiently distinct from each other, i.e., without any correlation and quark exchange effect. Thus, by dropping the exchange term and ignoring the Fermi motion effect, we are left with the collection of free nucleons in each nucleus,

$$\mathcal{F}_2^{^3\mathrm{He}}(x,Q^2)|_{\mathcal{I}=0} = 2\mathcal{F}_2^p(x,Q^2)+\mathcal{F}_2^n(x,Q^2), \tag{27}$$

$$\mathcal{F}_2^{^3\mathrm{H}}(x,Q^2)|_{\mathcal{I}=0} = \mathcal{F}_2^p(x,Q^2)+2\mathcal{F}_2^n(x,Q^2). \tag{28}$$

Equations (27) and (28) can be simultaneously solved; therefore, the free proton and neutron structure functions will be determined,

$$\mathcal{F}_2^p(x,Q^2) = \tfrac{1}{3}\big[2\mathcal{F}_2^{^3\mathrm{He}}(x,Q^2)|_{\mathcal{I}=0} - \mathcal{F}_2^{^3H}(x,Q^2)|_{\mathcal{I}=0}\big], \tag{29}$$

$$\mathcal{F}_2^n(x,Q^2) = \tfrac{1}{3}\big[2\mathcal{F}_2^{^3\mathrm{H}}(x,Q^2)|_{\mathcal{I}=0} - \mathcal{F}_2^{^3\mathrm{He}}(x,Q^2)|_{\mathcal{I}=0}\big]. \tag{30}$$

In the QEM we take the nucleon radius $b = 0.8$ fm because of the charge radius for ^{3}He nucleus and ^{3}H is about 1.68 fm and 1.56 fm respectively [70], which corresponds to $b = 0.837$ and $b = 0.780$, fm. Therefore, $b = 0.8$ fm is a good choice. In our model, for each flavor, there are two free parameters, which are the quark mass, m_q, and their binding energies, ϵ_0^q, where their values physically have to be around 200 MeV with respect to the mass of the proton [11,17,18,23]. We take their numerical values to be $m_q = M_{\mathcal{N}}/3$ and $\epsilon_0^q = m_q/2$, where the index q indicate the $\mathcal{U}$-type or $\mathcal{D}$-type constituent quarks. On the other hand, as it has been shown in the previous works, the final results are not very sensitive to these parameters as far as they are chosen in the above range. Our model did not work well and not good enough as $x \to 1$, especially, for the nucleus targets, because by considering the leading-order expansion of the nuclear wave function in QEM the Fermi motion effect has been ignored by both bound and free nucleons.

IV. RESULT AND DISCUSSION

In this research paper, I calculate the various parton distribution functions inside the bound nucleons of light nuclei by using the convolution method, Eq. (1), to draw the hadronic structure functions of free and bound proton and neutron out by presuming a nucleon as the bound state of constituent quarks. In high-energy physics, it is very important to study the partonic contents of the nucleon and nucleus to calculate the structure function of the nucleus like helium-3 and tritium and the bound nucleon by using the different parton distribution functions.

The concept of the CQ as the building block of the nucleons, in which the CQ can be assumed as a composite object as well as the quark exchange formalism, has been used to extract the different parton distribution functions like PL valence-up and -down quarks, PL sea quarks, and PL gluons inside the bound nucleon to shed some light on the subject of the structure functions of the bound nucleon and the light nuclei like helium-3 and tritium. The constituent quark is a dressed-up quark surrounded by clouds of PL valence quarks, PL sea quarks, and PL neutral gluons. Thus, a constituent quark obtains its own structure by dressing a PL valence quark with the gluons and the quark-antiquark pairs in the framework of QCD. The structure function of the constituent quark is reformulated with the new parameters at the energy scale of $Q^2 = 4$ GeV^2. There are a lot of available and relevant data at this scale of energy, which, therefore, is one of our reasons that this scale has been chosen. Especially, the neutron to the proton structure-function ratio as well as helium-3 to tritium could be calculated in order to compare with the recent experimental data of the ratio of structure function of ^{3}He to ^{3}H at $Q^2 = 4$ GeV^2 from the JLab experiment Ref. [71]. Moreover, at this value of Q^2, it is possible to compare our results with various theoretical outcomes like the one of Bissey *et al.* [16].

Thus, in the first step, I tried to determine the density distributions of the $\mathcal{U}$-type and the $\mathcal{D}$-type constituent quarks inside the bound nucleon from a completely consistence realistic formalism, where for this purpose the quark exchange model formalism has been chosen. By using these

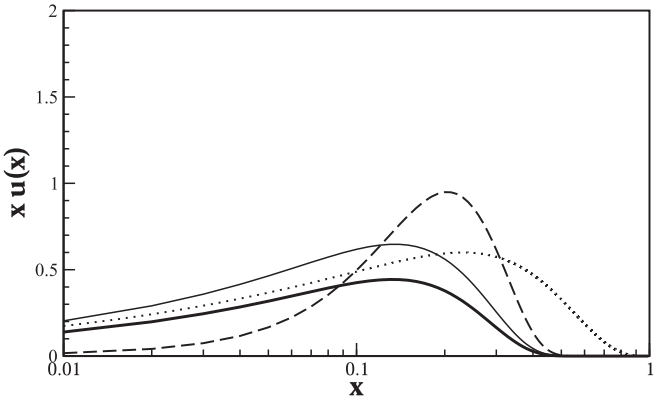

FIG. 1. The PL valence-up quarks $u_{\rm val}(x)$ (the heavy full curve), Eq. (16), the constituent up quarks $G_{\mathcal{U}/N}$ (dashed curve), Eq. (14), in the ^{3}He for the $(m_u,\ \epsilon_0^u)$ pairs of $(\frac{1}{3}M_N,\ \frac{1}{2}m_u)$ and $b = 0.8$ fm at $Q^2 = 4$ GeV^2. I have also shown the PL up-quark distribution of the free nucleon (the full curve) and the predictions of GRV's free valence-up quark distributions (dotted curve) at $Q^2 = 4$ GeV^2 [63].

densities, the different PDFs inside the bound nucleon will be calculated.

I start by presenting the extracted PL valence quark distributions inside the bound nucleon (the heavy full curves), the PL valence quark distribution of the free nucleon (the full curve), and $\mathcal{U}$-type and $\mathcal{D}$-type constituent quarks (dashed curves) of up- and down-quarks for ^{3}He in Figs. 1 and 2, respectively. The former were extracted from the convolution of the constituent quark inside the bound nucleon by using Eq. (1) for $q = u_{\rm val}$ and $q = d_{\rm val}$. It should be pointed out that, in this paper, the probability distributions of the constituent quark, i.e., $G_{\mathcal{U}/N}(y, Q_0^2)$ and $G_{\mathcal{D}/N}(y, Q_0^2)$ (the dashed curves in Figs. 1 and 2, respectively), have been obtained by using the QEM according to the procedure that is explained in Appendix. This model is a realistic model; therefore, it produces more reliable results than with the nonrelativistic

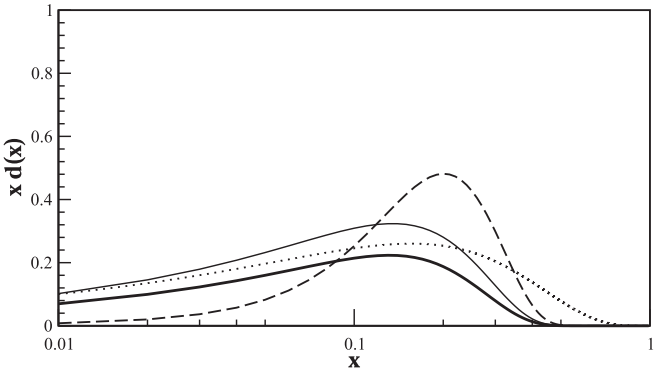

FIG. 2. The same as the Fig. 1 but for the d quarks. The PL valence-down quarks $d_{\rm val}(x)$ (the heavy full curve), Eq. (17), the constituent up-quarks $G_{\mathcal{D}/N}$ (the dashed curve), Eq. (15), in the ^{3}He for the $(m_d,\ \epsilon_0^d)$ pairs of $(\frac{1}{3}M_N,\ \frac{1}{2}m_d)$ and $b = 0.8$ fm at $Q^2 = 4$ GeV^2. I have also shown the PL down-quark distribution of the free nucleon (the full curve) and the predictions of GRV's free valence down-quark distributions (dotted curve) at $Q^2 = 4$ GeV^2 [63].

model of Isgur and Karl [72–74] or the algebraic model of Bijkar *et al.* [75–77]. They are both based on field-theoretical approaches and we made a comparison among these models and the present model in Ref. [56].

In the QEM formalism, for each constituent quark flavor, there are two parameters that have to be fixed in order to predict the parton densities inside the bound nucleon. In order to construct our constituent quark distribution functions, I take the proton parton distribution functions that can be provided by the GRV's (Glück *et al.*) valence quark distributions [63], which are extracted by performing the next-to-leading-order QCD calculations on $F_2^P(x, Q^2)$, and their results have a very good fit with respect to the available data in the whole (x, Q^2) plane, therefore; their parton distributions at the energy scale $Q^2 = 4$ GeV^2 should be reliable. In this scale of energy, the PL valence-up and -down quark distributions become closer to those of GRV, especially, for the $x < 0.1$. Also, it is interesting that the shape of the distributions has the same pattern of those GRV. It is acceptable because in the small-x-region one we are dealing with other nuclear effects like the shadowing effect, which is not included in the present model. So in the small-x region, it is expected that the nuclear distributions are close to those of GRV parametrization which describe the free nucleon distributions. Thus, I just take the nuclear effect of the quark exchange between bound nucleons into account where it is important in the $0.2 < x < 0.7$ region. But as $x \to 1$, the behavior of the present distributions is different from those of GRV's, mainly for the nuclear targets, in which the effect of Fermi motion of bound nucleon inside the nucleus has been ignored by using the leading-order expansion of the nuclear wave function. Therefore, as is obvious from Fig. 1, because of the binding and the Fermi motion effect, it is expected that for the large x the PL valence-up and -down quark distributions behave differently with respect to those have been fitted to produce the free-nucleon structure function, i.e., GRV.

On the other hand, it is obvious that since $\mathcal{U}$-type and $\mathcal{D}$-type constituent quarks have different momentum density distribution in the QEM, Eqs. (A10) and (A11), the PL valence-up and -down quark distributions take a different shape through using the CQM formalism, i.e., Eq. (1). But in the case of the sea quarks or the gluon distributions in the nuclear systems, there is no flavor dependent so the single distributions for the sea quarks or gluons will be obtained. The flavor independence of the gluon is that in the ACMP constituent quark formalism, there is no difference between the PL gluon distribution inside the $\mathcal{U}$-type constituent quark and the $\mathcal{D}$-type constituent quark, because in the Eq. (1), the same functional form for both of them have been derived; therefore, the gluon distributions are flavor blinded. It is obvious that by using the convolution methods the distributions of PL up- and down-valence quarks produce a very reliable outcome rather those of constituent quark, which will give better results in the case of the ratios of the structure functions of the neutron to the proton as well as the ratio of the helium-3–to-tritium structure functions.

In Fig. 3, the sea-quark distributions have been presented which calculated through Eq. (1) by using the $\mathcal{U}$-type and the $\mathcal{D}$-type constituent quark distributions of QEM (the full

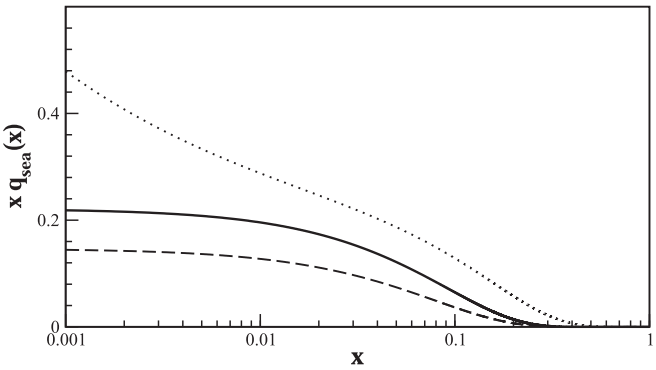

FIG. 3. The PL sea quarks $q_{\rm sea}(x)$ (the full curve), Eq. (18), in the ^{3}He for the $(m_q,\ \epsilon_0^q)$ pairs of $(\frac{1}{3}M_N,\ \frac{1}{2}m_q)$ and $b = 0.8$ fm at $Q^2 = 4$ GeV^2. The dashed curve is our previous results from Ref. [57] at $Q^2 = 0.34$ GeV^2. I have also shown the predictions of the free GRV's isospin average sea quarks (dotted curve) at $Q^2 = 4$ GeV^2 [63].

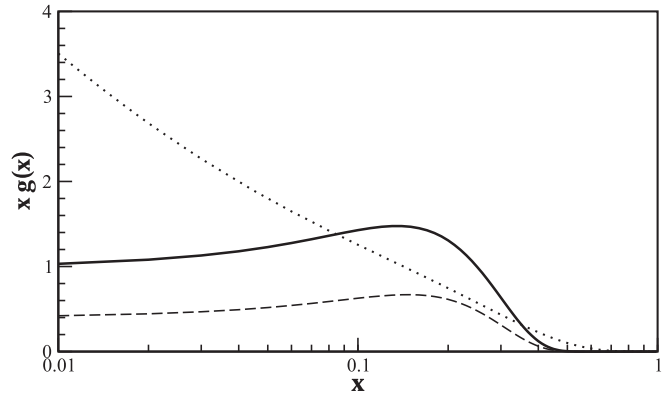

FIG. 4. The PL gluons $g(x)$ (the full curve), Eq. (19), in the ^{3}He for the $(m_q,\ \epsilon_0^q)$ pairs of $(\frac{1}{3}M_N,\ \frac{1}{2}m_q)$ and $b = 0.8$ fm at $Q^2 = 4$ GeV^2. I also added to the present figure our previous results from Ref. [57] at $Q^2 = 0.34$ GeV^2 (dashed curve). The dotted curve is the GRV's gluon distribution in the free nucleon at $Q^2 = 4$ GeV^2 [63].

curve). The parameters of the calculations, i.e., the quark mass, m_q, the quark binding energy, ϵ_q, the nucleon's radius, b, and the scale of energy, Q_0^2, are the same as Figs. 1 and 2. In the previous works that the quark exchange model has been used to explain the results of the DIS experimental data especially the EMC ratios of an $A = 3$ isoscalar target [10] and the ^{3}He and ^{3}H nuclear structure functions [22], only the exchange of the $\mathcal{U}$-type and $\mathcal{D}$-type constituent quark among the nucleons bound in the nucleus have been considered and the existence as well as the exchange of the sea quarks and the gluons have been ignored due to the complexity of the calculations. But in the present work, the important role of the sea quarks in the structure functions of the bound nucleons and nuclear targets in the high-energy physics have been considered through the application of the QEM formalism in the context of the CQM framework, so the obtaining results are in a very good agreement with the available and relevant data, see Figs. 7 and 8. On the other hand, as pointed out before there is no flavor dependence in the case of the sea quarks, $q_{\rm sea}(x, Q_0^2)$, and the gluons, $g(x, Q_0^2)$, so for all types of sea-quark distributions, namely $q_{\rm sea} = u_{\rm sea}, d_{\rm sea}, \bar{u}_{\rm sea}, \bar{d}_{\rm sea}, s_{\rm sea}$, and $\bar{s}_{\rm sea}$, and gluon distributions a single distribution inside ^{3}He or ^{3}H nucleus have been extracted. The dashed curve is the PL sea-quark distribution for the hadronic scale of energy, i.e., $Q_0^2 = 0.34$ GeV^2, which is presented for comparison [57]. It could be seen that, as the energy values become higher, the PL sea-quark distributions grow, which means that more quark-antiquark pairs have been created and the momentum of the nucleon should be shared between them, so the contribution of the PL valence quarks decreases and that of PL sea quarks increases. Also, it should be mentioned that the free-nucleon GRV's sea quarks are flavor dependent, but for comparison, I have plotted their isospin average distributions in Fig. 3 (the dotted curve), so the inconsistency between our results and those of the GRV should be considered as qualitative in nature.

In Fig. 4, I have plotted the results of the calculations for the PL gluon distributions (the full curve), $g(x, Q^2)$, which have been calculated through Eq. (1) by taking $q = g$ with the same value of parameters like b, Q_0^2, m_q, and ϵ_0^q of Fig. 3 along with the GRV's free-nucleon gluon distribution function (the dotted curve) at $Q^2 = 4$ GeV^2. Like Fig. 3, the previous result at the energy scale of $Q_0^2 = 0.34$ GeV^2 (dashed curve) have been presented for comparison. The effect of the presence of the gluons in the quark exchange model is considerable, as will be shown in the following results. I have plotted GRV's isospin average gluon distributions in Fig. 4 (dotted curve). An interesting point is that in the $0.1 < x < 0.4$ region, the bound gluon distribution inside the nucleon is larger than the GRV free-nucleon gluon distributions at the high energy scale and the behavior of the gluon in the small-x region differs from those of the free nucleon. It should be noted that our sea quark and gluon distributions have been calculated for the bound nucleons so it is natural that the behavior of these distributions is different from those of the "free nucleon." The functional form of the gluon distributions inside bound nucleon, i.e., $\Phi_{g/\rm CQ}(x)$, has been determined through the total amount of the momentum of the nucleon which has been carried by the gluons. Thus, the shape of these distributions has been imposed from these physical sum rules. Also the distributions presented in Figs. 3 and 4 are for two values of $Q^2 = 0.34$ GeV^2 and 4 GeV^2; therefore, it is obvious that by increasing the energies, the sea quark and gluon distributions have been increased, especially in the small-x regions.

In Fig. 5, the ratios of the bound PL valence-up and -down quark densities to those of the valence-up and -down quark distributions in the free nucleon are shown by the dash-dotted and dashed curves, respectively. The full curve is the PL valence quark distributions, $q_{\rm val} = u_{\rm val} + d_{\rm val}$. The filled squares are the experimental data [78] and the small dashed curve is the theoretical predictions of Afnan *et al.* [16] for helium-3 and the tritium, which are shown just for comparison. In the present calculations, it is clearly obvious that the EMC-type ratio of the PL valence quark has the same pattern as the one that has been obtained for the EMC-type ratio of the bound nucleon. It should be noted that the bound PL valence quark distributions are smaller than the free valence quark

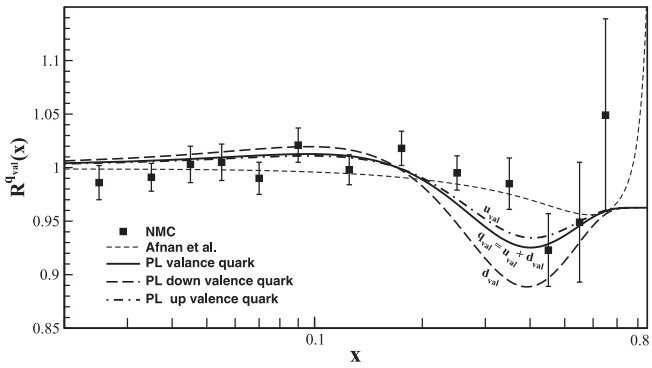

FIG. 5. The EMC ratios of the bound PL valence-up and -down quarks to the free valence quark in the helium-3 nucleus. The full curve is the PL valence quark distributions, $q_{\rm val} = u_{\rm val} + d_{\rm val}$ and the dash-dotted and dashed curves are the same ratios but for the PL up- and down-quarks, respectively. The filled squares are the experimental data [78]. The small dashed curve is the theoretical result [16] for helium-3 and tritium, which is presented for comparison.

distributions in the interval $0.15 < x < 0.65$. It is expected because, as explained before, in the mentioned region the quark exchange effect between the bound nucleons is present and causes a shift in the CQ momentum distributions. Also one can conclude that the effect of the quark exchange is reliable for the PL valence-down quarks rather than the PL valence-up quarks.

The EMC-type ratios of ^{3}He and ^{3}H nuclei, Eqs. (24) and (25), are presented in Fig. 6 for the nucleon radius $b = 0.8$ fm, (the full curves). It should be mentioned that the original EMC effect is the ratio of the nuclear structure functions to those of the deuteron. So in the present model, Eqs. (24) and (25) are for the ratio of the bound-nucleon structure function to the corresponding free nucleon; therefore, it is not calculating

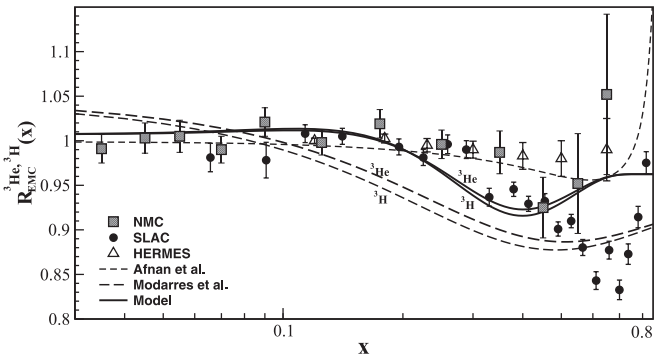

FIG. 6. The EMC ratios of the ^{3}He and ^{3}H nuclei, Eqs. (24) and (25), for $b = 0.8$ fm. The full curves are from present calculations by taking into account the contributions of the PL sea quarks and the PL gluons in the structure functions at $Q^2 = 4$ GeV^2. The dashed curves are the same ratio, but only the $\mathcal{U}$-type and $\mathcal{D}$-type constituent quarks are included [22]. The empty triangles are the data from HERMES helium-3 analysis Refs. [13,14], The filled circles are the SLAC experiment for the ^{56}Fe nucleus [12], the filled squares are taken from Ref. [78], and the small dashed curve is those of the theoretical approach of Afnan *et al.* [16].

the ratio addressed in the experimental analysis. Of course, our results here are a good indication of the goodness of the ACMP constituent quark exchange model to explain the available data.

The EMC ratio of ^{3}He and ^{3}H nuclei in which just $\mathcal{U}$-type and $\mathcal{D}$-type constituent quarks, i.e., $G_{\mathcal{U}/N}(y, Q_0^2; A_i)$ and $G_{\mathcal{D}/N}(y, Q_0^2; A_i)$, have been considered in the nuclear structure functions (dashed curves), also presented from Ref. [22]. Thus, by comparing the results of the present study with the previous one, it is obvious that by taking the different parton density distributions such as the PL valence-up and -down quarks, PL sea quarks, and PL neutral gluons into account, reliable ratios have been obtained in the discussed region. The empty triangles are the data from HERMES helium-3 analysis that is a combinations of helium-3, the deuterium, and the proton cross sections $\mathcal{R} = \mathcal{F}_2^{^3\rm He}/(F_2^d + F_2{}^p)$, and they have been taken from Refs. [13,14]. The filled circles are the Stanford linear accelerator center (SLAC) experimental data for the ^{56}Fe nucleus [12], the filled squares are taken from Ref. [78], and the small dashed curve is those of Afnan *et al.* [16] for the helium-3 and the tritium nuclei. Afnan *et al.* have used the spectral function and convolution approaches with inclusion of the Fermi motion effect to get their outcomes. Our results for the small-x region and the valence domains are in a good agreement with both the experimental data and theoretical results, but they are not comparable for the deep valence region, $x > 0.7$, in which the Fermi motion is an important effect while has been ignored in the present calculations. Thus, as is obvious, the results fall short off representing experimental data. One should note that the results are a good indication of the goodness of the model to explain data. The outcomes of the model for large x not surprising, for it is a well-established fact that in this study, as in our previous works [22,57], the exchange term has been approximately calculated due to the leading-order expansion of the nuclear wave function, $\chi(\mathbf{p}, \mathbf{q})$; i.e., discarding the Fermi motion. In fact, as I discuss completely in Appendix, in the QEM formalism the state of the nucleus with three nucleons has been defined as follows [11]:

$$|A_i = 3\rangle = (3!)^{-1/2}\, \chi^{\alpha_1\alpha_2\alpha_3} \mathcal{N}^\dagger_{\alpha_1} \mathcal{N}^\dagger_{\alpha_2} \mathcal{N}^\dagger_{\alpha_3} |0\rangle. \qquad (31)$$

The nuclear wave function $\chi^{\alpha_1\alpha_2\alpha_3}$ could be defined as the center-of-mass motion of the three nucleons and we write it as follows:

$$\chi^{\alpha_1\alpha_2\alpha_3} = \chi(\mathbf{P}, \mathbf{q}) D(\alpha_1, \alpha_2, \alpha_3; A_i), \qquad (32)$$

where $D(\alpha_1, \alpha_2, \alpha_3; A_i)$ are the C-G coefficients for the three-nucleon system. It should be noted that the effect of the Fermi motion in the nuclear targets are predominant at $x > 0.65$, as obvious from the data and theoretical results of Fig. 6 and Refs. [12,16,26]. I hope to consider the effect of the Fermi motion in our future works to the constituent quark exchange formalism by taking into account the variation of the nuclear wave function in the configuration space [56]. In Ref. [16], it has been shown that the ratio of the EMC ratio of helium-3 to tritium should be approximately equal to unity, where our results in the present figure are in a good agreement with this prediction.

In the next two figures, the ratio of the neutron to the proton structure functions as well as the helium-3–to–tritium structure functions are shown as a function of x at $Q^2 = 4$ GeV^2 and we compare them with the available data to check the validity of our model. It is good to present the outcomes for the ratio of the helium-3–to–tritium structure-function ratio $\frac{F_2^{^3\mathrm{He}}}{F_2^{^3\mathrm{H}}}$. The nuclear target structure functions like ^{3}He and ^{3}H in the constituent quark exchange formalism have been calculated by Eqs. (22) and (23). Using the same numerical values as the one I have chosen in Fig. 1, the mentioned ratios will be obtained.

In Fig. 7, the full curve shows the ratio of the ^{3}He-to-^{3}H structure functions and the dashed curve represents the same ratio but only the $\mathcal{U}$-type and $\mathcal{D}$-type constituent quark distributions $G_{\mathcal{U}/N}(y, Q_0^2)$ and $G_{\mathcal{D}/N}(y, Q_0^2)$ have been considered to calculate the nuclear structure functions. For the purpose of comparing our results with the available data and checking the validity of the present calculations, the expected ratios that have been predicted by using the kinematics of the proposed 11-GeV JLab experiment [15,16,71] (the filled circles) also have been included in Fig. 7. The results are in excellent agreement with the prediction as was expected, because in the present calculations the role of the PL sea quarks and the PL gluons have been considered through using the convolution relation of constituent quarks, i.e., Eq. (1). I achieved a very good agreement between the results of the present calculations and the experimental data for the ratio of the helium-3–to–tritium structure function in the valence region, in which the model works properly, so the dashed curve has been modified. Notice that in the present calculation the Fermi motion has been ignored; therefore, the results are not close to the experimental data for $x > 0.7$.

Finally, in Figs. 8(a) and 8(b) I have plotted the ratio of the neutron to the proton NLO structure functions, $\frac{F_2^n}{F_2^p}$, vs x at $Q^2 = 4$ GeV^2. The form of the various PL parton distribution functions inside the bound nucleon has been defined in Eqs. (16)–(19). By taking those relations, along with the same numerical values as the ones that have been used in Fig. 1, this ratio has been calculated via Eqs. (30) and (29). The full curve (dashed-double-dotted curve) is the mentioned ratio with (without) contributions of the sea-quark and gluon distributions to calculate the nucleon structure functions.

Considering the PL sea quarks and the PL gluons to the quark exchange model calculations in the context of the ACMP constituent quark formalism has improved the mentioned ratio very well for the small and the deep-valence x region such that a very good agreement between our results and both the experimental data and the theoretical prediction has been obtained. It should be mentioned that our ratio is for the bound nucleons so the difference between our results and the experimental data in the large-x region is because we ignored the Fermi motion effect in QEM. The dashed

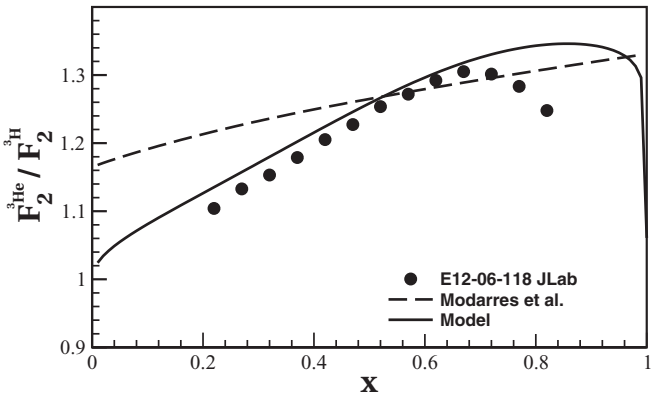

FIG. 7. The ratios of the structure functions of helium-3, $\mathcal{F}_2^{^3\mathrm{He}}(x, Q^2)$, to tritium, $\mathcal{F}_2^{^3\mathrm{H}}(x, Q^2)$, for $b = 0.8$ fm at $Q^2 = 4$ GeV^2. The full curve is based on the CQM in which the PL sea-quark and the PL gluon densities have been considered in the calculations and the dashed curve is the same ratio from Ref. [22] in which the sea quarks and the gluons are not taken into account. The circle points are the experimental data from Refs. [16,71].

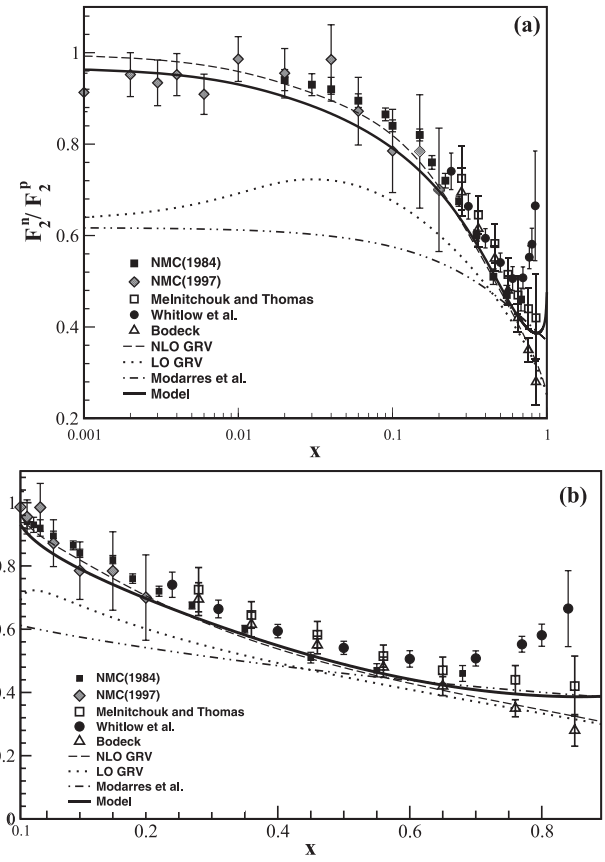

FIG. 8. (a) The ratio of the neutron to the proton NLO structure functions, $\frac{F_2^n}{F_2^p}$, as a function of x at $Q^2 = 4$ GeV^2 (the full curve). I have also shown the same ratio but without the role of the sea quarks and the gluon (the dash-dotted curve). The dashed curve (dotted curve) is the prediction of GRV's structure-function ratios with (without) the sea quarks and the gluons. The experimental data are from Whitlow *et al.* [79], Melnitchouk and Thomas [80], Bodek *et al.* [81], and NMC [12,82]. The results are plotted for $x > 0.001$. (b) The same as Fig. 8(a), i.e., the ratio of the neutron to the proton NLO structure functions, $\frac{F_2^n}{F_2^p}$, as a function of x at $Q^2 = 4$ GeV^2 but results are plotted for $x > 0.1$.

curve is the full NLO GRV F_2^n/F_2^p ratio and the dotted curve is the same ratio but without the gluon and the sea-quark distributions [63]. It should be noted that I assumed the isospin symmetry. The presented data are for $Q^2 = 3$–7 GeV^2.

V. CONCLUSION

In conclusion, I have used quark exchange formalism to produce the $\mathcal{U}$-type and $\mathcal{D}$-type constituent quark distribution functions to be used as the constituent quark distributions to the ACMP constituent quark model. The constituent quark obtains their own structure by grabbing a valence quark with the quark-antiquark pairs and the neutral gluons. I have calculated and reparameterized the constituent quarks structure functions, i.e., $\Phi_{q/cQ}$, at energy scale $Q^2 = 4$ GeV^2. The convolution theorem has been used to calculate the PL up-valence quark, $u_{\rm val}$, the PL down-valence quark, $d_{\rm val}$, the PL sea quark, $q_{\rm sea}$, and the PL gluon, g, where they are the partonic structure of the bound nucleons. I have explicitly shown the results of the present calculation to compare them with the available and relevant experimental data as well as with the prediction of the theoretical outcomes. It has been found that our results are in a good agreement with the experimental data. Also, our derived structure functions are more reliable and realistic because in the present calculations, the contribution and the role of the sea quark and the gluon distributions to obtain the structure functions of nucleons and nuclear targets, especially for $x < 0.1$ have been considered, so the ratio of the structure functions pass to the experimental data very closely.

The model can be improved by considering the Fermi motion effect explicitly in the constituent quark distributions, i.e., considering the full overlap integral in the context of the quark exchange model by taking the full nuclear wave function into account rather than the leading-order expansion of the nuclear wave function; moreover, the results will be improved by evaluating the connected three-body diagram of the quark exchange, which has been ignored in the present calculations. It should be pointed out that the unintegrated parton distribution function in the nuclei has a major role [31] and it was very recently used for the case of $A = 6$ nuclei [30], in which the result was noticeable. I hope that in our future works we add this point to the helium-3 and the tritium nucleus structure functions in order to calculate the very small-x behavior of the structure functions of ^{3}He and ^{3}H nuclei in the framework of the constituent quark exchange model.

ACKNOWLEDGMENT

I thank the Research Council of Razi University for the grants provided.

APPENDIX: DERIVATION OF THE $\mathcal{U}$-TYPE AND $\mathcal{D}$-TYPE CONSTITUENT QUARK DISTRIBUTIONS FROM QEM

In this Appendix, I describe the derivation of the constituent quark distribution functions from QEM [11]. In this formalism, it is considered that the exchange of the quarks between the bound nucleons inside the nucleus may cause a displacement in the momentum distribution of their partons relative to partons inside the free nucleon. In this Appendix, the procedure leads to the explanation of this calculation and it was shown that the shift and exchange of the partons among bound nucleons contributes to the parton distributions functions. To this end, it assumed that the nucleon state be composed of three constituent quarks, where each of them has its own special quantum numbers, such as the spin, isospin, and the color factor, which have been collectively shown by the index μ.

The constituent quark state can be defining by the constituent quark creator operator, $(cq)^\dagger$, as follows:

$$|cq\rangle = (cq)^\dagger_\mu |0\rangle \tag{A1}$$

and equivalently for the nucleon kind $\mathcal{N}$ made of three constituent quarks, cq. It can be written [11,19–22],

$$|\mathcal{N}\rangle = \mathcal{N}^\dagger_\alpha |0\rangle = \frac{1}{\sqrt{3!}} \mathcal{N}^{\mu_1\mu_2\mu_3}_\alpha (cq)^\dagger_{\mu_1} (cq)^\dagger_{\mu_2} (cq)^\dagger_{\mu_3} |0\rangle. \tag{A2}$$

In this equation the indices α_i (μ_i) describe the nucleon (CQ) states $\{\mathbf{P}, \mathcal{M}_S, \mathcal{M}_T\}$ ($\{\mathbf{k}, m_s, m_t, c\}$) [note that M_T (m_t) $= +\frac{1}{2}$ and $-\frac{1}{2}$ for the proton (up constituent quark) and the neutron (down constituent quark), respectively]. The creation operator for the constituent quark (nucleons) is shown as $cq^\dagger_\mu$ ($\mathcal{N}^\dagger_\alpha$) in which μ (α) is a state index. It should be pointed out that, as a convection, repeated indices means a summation over those indices and also integration over $\mathbf{k}$. In Eq. (A2), $\mathcal{N}^{\mu_1\mu_2\mu_3}_\alpha$ is a totally antisymmetric nucleon wave function and is written as follows:

$$\begin{aligned}\mathcal{N}^{\mu_1\mu_2\mu_3}_\alpha &= D(\mu_1, \mu_2, \mu_3; \alpha_i) \times \delta(\mathbf{k_1} + \mathbf{k_2} + \mathbf{k_3} - \mathbf{P}) \\ &\quad \times \Phi(\mathbf{k_1}, \mathbf{k_2}, \mathbf{k_3}, \mathbf{P}),\end{aligned} \tag{A3}$$

in which $\Phi(\mathbf{k_1}, \mathbf{k_2}, \mathbf{k_3}, \mathbf{P})$ describe the nucleon wave function in terms of the constituent quarks. Also, it should be mentioned that because the quark exchange model is a nonrelativistic framework, it would be possible to separate the center-of-mass motion of the nucleon from the motion of its constituent quarks. Thus, by considering this point, there is some simplifying of the calculation in the quark exchange model, for which the nucleon wave function is approximated by a Gaussian form:

$$\begin{aligned}&\Phi(\mathbf{k_1}, \mathbf{k_2}, \mathbf{k_3}, \mathbf{P}) \\ &= \left(\frac{3b^4}{\pi^2}\right)^{\frac{3}{4}} \exp\left[-\frac{b^2}{2}\left(k_1^2 + k_2^2 + k_3^2 - \frac{P^2}{3}\right)\right],\end{aligned} \tag{A4}$$

($b \simeq$ nucleon radius). The $D(\mu_1, \mu_2, \mu_3; \alpha_i)$ part in the Eq. (A3) is the abbreviation for the products of the color factor $\epsilon_{c_1c_2c_3}$ and four Clebsch-Gordon coefficients $C^{j_1 j_2 j}_{m_1 m_2 m}$, so it is written as the following form:

$$\begin{aligned}D(\mu_1, \mu_2, \mu_3; \alpha_i) = \frac{1}{\sqrt{3!}} \epsilon_{c_1c_2c_3} \frac{1}{\sqrt{2}} \sum_{s,t=0,1} C^{\frac{1}{2}s\frac{1}{2}}_{m_{s_\sigma} m_s M_{S_{\alpha_i}}} \\ \times C^{\frac{1}{2}\frac{1}{2}s}_{m_{s_\mu} m_{s_\nu} m_s} C^{\frac{1}{2}t\frac{1}{2}}_{m_{t_\sigma} m_t M_{T_{\alpha_i}}} C^{\frac{1}{2}\frac{1}{2}t}_{m_{t_\mu} m_{t_\nu} m_t}.\end{aligned} \tag{A5}$$

Now the nucleus state with $A_i = 3$ can be defined by using the above nucleon creation operator and the completely

antisymmetric nuclear wave function, $\chi^{\alpha_1\alpha_2\alpha_3}$, as follows:

$$|A_i = 3\rangle = (3!)^{-1/2}\, \chi^{\alpha_1\alpha_2\alpha_3} \mathcal{N}^\dagger_{\alpha_1}\mathcal{N}^\dagger_{\alpha_2}\mathcal{N}^\dagger_{\alpha_3}|0\rangle. \tag{A6}$$

Afnan *et al.* [16] show that there is a degree of freedom in which the choice of the nucleon-nucleon potential does not affect the EMC ratio, which has been proved in several works where the EMC effect have been studied [22,26,27]. In fact, the binding energy and nuclear effects cause the EMC ratio for $0.2 < x < 0.8$, which is the valence region. The different potentials are responsible for the same binding energy of the nucleons inside the nucleus so the change of the potential does not change the binding energy; therefore, the EMC ratio, as has been checked by various works, does not depend on the potential's model to describe the nuclear systems. In other words, the EMC ratio is rather independent from the potential model if the latter is realistic. Recently, we have used the Malfliet-Tjon V potential [26] to calculate the wave function of the three-nucleon systems in the coordinate space in order to calculate the EMC effect. The results were the same as that in which the Reid or AV18 potential have been used. Thus, one can conclude that the EMC ratio is not affected by the change of the nucleon-nucleon potential.

Also, it worth noting that, for the three-nucleon systems the nuclear density is sufficiently low; therefore, it should be correct to ignore the possibility of simultaneous quark exchange among all three nucleons. The nuclear wave function $\chi^{\alpha_1\alpha_2\alpha_3}$ could be defined as the center-of-mass motion of the three nucleons and write it by this assumption as follows:

$$\chi^{\alpha_1\alpha_2\alpha_3} = \chi(\mathbf{P},\mathbf{q})D(\alpha_1,\alpha_2,\alpha_3;A_i), \tag{A7}$$

where $D(\alpha_1,\alpha_2,\alpha_3;A_i)$ are the C-G coefficients for the three nucleons as the one in Eq. (A5), i.e.,

$$D(\alpha_1,\alpha_2,\alpha_3;A_i) = \frac{1}{\sqrt{2}}\sum_{S,T=0,1} C^{\frac{1}{2}S\frac{1}{2}}_{M_{S_{\alpha_1}}\mathcal{M}_S M_{S_i}} C^{\frac{1}{2}\frac{1}{2}S}_{M_{S_{\alpha_2}}M_{S_{\alpha_3}}\mathcal{M}_S} \times C^{\frac{1}{2}T\frac{1}{2}}_{M_{T_{\alpha_1}}\mathcal{M}_T M_{T_i}} C^{\frac{1}{2}\frac{1}{2}T}_{M_{T_{\alpha_2}}M_{T_{\alpha_3}}\mathcal{M}_T}. \tag{A8}$$

In order to extract the constituent quark distribution inside the bound nucleon of the nuclear system, the momentum density distributions is needed. The momentum distribution functions of a constituent quark with the fixed flavor and the nucleon isospin projection in the three-nucleon system can be written as

$$\rho_{\bar{\mu}}(\mathbf{k};A_i) = \frac{\langle A_i = 3|(cq)^\dagger_{\bar{\mu}}(cq)_{\bar{\mu}}|A_i = 3\rangle}{\langle A_i = 3|A_i = 3\rangle}. \tag{A9}$$

We used the sign bar to indicate that there is no summation on $\mathcal{M}_T$, m_t and integration over $\mathbf{k}$ on the repeated index μ. The details of the calculations of $\langle A_i = 3|A_i = 3\rangle$ and $\langle A_i = 3|(cq)^\dagger_{\bar{\mu}}(cq)_{\bar{\mu}}|A_i = 3\rangle$ can be found in Ref. [22].

Now by performing all summations on the free repeated indices in Eq. (A9), but for fixed $\mathcal{M}_\mathcal{T} = \frac{1}{2}$ and $-\frac{1}{2}$, the momentum density distributions of the ^{3}He and the ^{3}H nuclei could be calculated, respectively ($\mathcal{M}_\mathcal{T}$ is the three-nucleon system isospin projection) [22]:

$$\rho^{^3\mathrm{He}}(k) = \left[2\mathcal{A}(k) + \frac{2}{9}\mathcal{B}(k) + \frac{4}{9}\mathcal{D}(k)\right]\left[1 + \frac{9}{8}\mathcal{I}\right]^{-1}, \tag{A10}$$

$$\rho^{^3\mathrm{H}}(k) = \left[\mathcal{A}(k) + \frac{1}{9}\mathcal{B}(k) + \frac{4}{9}\mathcal{C}(k) - \frac{2}{9}\mathcal{D}(k)\right]\left[1 + \frac{9}{8}\mathcal{I}\right]^{-1}, \tag{A11}$$

with

$$\int \rho^{^3\mathrm{H}}(k)d\mathbf{k} = \frac{1}{2}\int \rho^{^3\mathrm{He}}(k)d\mathbf{k}. \tag{A12}$$

In Eqs. (A10) and (A11), $\mathcal{A}(k)$, $\mathcal{B}(k)$, $\mathcal{C}(k)$, and $\mathcal{D}(k)$ are the direct and exchange integrals calculated from the three-nucleon wave function. The mentioned terms are as follows:

$$\mathcal{A}(k) = \left[\frac{3b^2}{2\pi}\right]^{\frac{3}{2}} \exp\left[-\frac{3}{2}b^2k^2\right],$$

$$\mathcal{B}(k) = \left[\frac{27b^2}{8\pi}\right]^{\frac{3}{2}} \exp\left[-\frac{3}{2}b^2k^2\right]\mathcal{I}, \tag{A13}$$

$$\mathcal{C}(k) = \left[\frac{27b^2}{7\pi}\right]^{\frac{3}{2}} \exp\left[-\frac{12}{7}b^2k^2\right]\mathcal{I},$$

$$\mathcal{D}(k) = \left[\frac{27b^2}{4\pi}\right]^{\frac{3}{2}} \exp\left[-3b^2k^2\right]\mathcal{I}, \tag{A14}$$

and

$$\mathcal{I} = 8\pi^2 \int_0^\infty x^2\,dx \int_0^\infty y^2\,dy \int_{-1}^1 d(\cos\theta) \exp\left[-\frac{3x^2}{4b^2}\right] \times |\chi(x,y,\cos\theta)|^2, \tag{A15}$$

in which the exchange integral, i.e., $\mathcal{I}$, is the contribution of the nucleus wave function $[\chi(x,y,\cos\theta)]$ to the constituent quark momentum distributions [11]. It is assumed that if one takes $\mathcal{I} = 0$, it means that there is no exchange of the quarks between the nucleons inside the nucleus, so the nucleon can be taken as the free one. This procedure has been used to obtain the free-nucleon structure function to be used to calculate the EMC-type ratios.

By assuming the SU(6) symmetry, the constituent up- and down-quark distribution functions inside the three-nucleon systems can be obtained as the following relations:

$$\rho^{\mathcal{U}}(k) = \left[2\mathcal{A}(k) + \frac{2}{9}\mathcal{B}(k) - \frac{16}{27}\mathcal{C}(k) + \frac{28}{27}\mathcal{D}(k)\right] \times \left[1 + \frac{9}{8}\mathcal{I}\right]^{-1}, \tag{A16}$$

$$\rho^{\mathcal{D}}(k) = \left[\mathcal{A}(k) + \frac{1}{9}\mathcal{B}(k) - \frac{20}{27}\mathcal{C}(k) + \frac{26}{27}\mathcal{D}(k)\right] \times \left[1 + \frac{9}{8}\mathcal{I}\right]^{-1}, \tag{A17}$$

[1] J. J. Aubert *et al.*, Phys. Lett. B **105**, 322 (1983).

[2] M. Derrick *et al.* (ZEUS collaboration), Z. Phys. C **72**, 399 (1996); Phys. Lett. B **316**, 412 (1993); **407**, 402 (1997); J. Breitwag *et al.*, Eur. Phys. J. C **12**, 35 (2000); **7**, 609 (1999); S. Chekanov *et al.*, Phys. Rev. D **69**, 012004 (2004).

[3] T. Ahmed *et al.*, Nucl. Phys. B **439**, 471 (1995); A. Airapetian *et al.*, Phys. Lett. B **442**, 484 (1998); J. Ashman *et al.*, *ibid.* **206**, 364 (1988); Nucl. Phys. B **328**, 1 (1989); S. Aid *et al.*, *ibid.* **445**, 3 (1996).

[4] I. Abt *et al.* (H1 collaboration), Nucl. Phys. B **407**, 515 (1993); S. Chekanov *et al.* (ZEUS collaboration), Eur. Phys. J. C **21**, 443 (2001); C. Adloff *et al.* (H1 collaboration), *ibid.* **19**, 269 (2001); **21**, 33 (2001); **13**, 609 (2000); A. Aktas *et al.* (H1 Collaboration), Phys. Lett. B **598**, 159 (2004); **602**, 14 (2004).

[5] D. Adams *et al.*, Phys. Rev. D **56**, 5330 (1997); Phys. Lett. B **357**, 248 (1995); **329**, 399 (1994); B. Adeva *et al.*, *ibid.* **369**, 93 (1996); **302**, 533 (1993); Phys. Rev. D **58**, 112001 (1998).

[6] K. Abe *et al.* (E143 Collaboration), Phys. Rev. Lett. **78**, 815 (1997); **74**, 346 (1995); **75**, 25 (1995); Phys. Lett. B **364**, 61 (1995); Report No. Slac-Pub-95-6982 (1995); Phys. Rev. D **58**, 112003 (1998).

[7] P. L. Anthony, R. G. Arnold, H. R. Band, H. Borel, P. E. Bosted, V. Breton, G. D. Cates, T. E. Chupp, F. S. Dietrich, J. Dunne, R. Erbacher, J. Fellbaum, H. Fonvieille, R. Gearhart, R. Holmes, E. W. Hughes, J. R. Johnson, D. Kawall, C. Keppel, S. E. Kuhn, R. M. Lombard-Nelsen, J. Marroncle, T. Maruyama, W. Meyer, Z. E. Meziani, H. Middleton, J. Morgenstern, N. R. Newbury, G. G. Petratos, R. Pitthan, R. Prepost, Y. Roblin, S. E. Rock, S. H. Rokni, G. Shapiro, T. Smith, P. A. Souder, M. Spengos, F. Staley, L. M. Stuart, Z. M. Szalata, Y. Terrien, A. K. Thompson, J. L. White, M. Woods, J. Xu, C. C. Young, and G. Zapalac, Phys. Rev. Lett. **71**, 959 (1993); P. L. Anthony *et al.*, Nuovo Cimento A **107**, 2197 (1994); G. Cates, in *Proceeding of Spin96 Conference*, Vol. 253, edited by T. Ketel and P. Mulders, (World Scientific, Singapore, 1997); P. L. Anthony, R. G. Arnold, H. R. Band, H. Borel, P. E. Bosted, V. Breton, G. D. Cates, T. E. Chupp, F. S. Dietrich, J. Dunne, R. Erbacher, J. Fellbaum, H. Fonvieille, R. Gearhart, R. Holmes, E. W. Hughes, J. R. Johnson, D. Kawall, C. Keppel, S. E. Kuhn, R. M. Lombard-Nelsen, J. Marroncle, T. Maruyama, W. Meyer, Z. E. Meziani, H. Middleton, J. Morgenstern, N. R. Newbury, G. G. Petratos, R. Pitthan, R. Prepost, Y. Roblin, S. E. Rock, S. H. Rokni, G. Shapiro, T. Smith, P. A. Souder, M. Spengos, F. Staley, L. M. Stuart, Z. M. Szalata, Y. Terrien, A. K. Thompson, J. L. White, M. Woods, J. Xu, C. C. Young, and G. Zapalac, Phys. Rev. D **54**, 6620 (1996); P. L. Anthony *et al.*, Report No. Slac-Pub-7994, July 2000 (hep-ph/007248).

[8] L. L. Frankfurt and M. I. Strikman, Phys. Rep. **76**, 215 (1981); R. E. Taylor, Rev. Mod. Phys. **63**, 573 (1991); G. Piller and W. Wesie, Phys. Rep. **330**, 1 (2000); M. M. Sargsian *et al.*, J. Phys. G: Nucl. Part. Phys. **29**, R1 (2003).

[9] R. P. Feynman, *Photon Hadron Interactions* (Benjamin, New York, 1972); F. E. Close, *An Introduction to Quarks and Partons* (Academic Press, London, 1989); R. G. Roberts, *The Structure of the Proton* (Cambridge University Press, New York, 1993).

[10] M. Betz, G. Krein, and Th. A. J. Maris, Nucl. Phys. A **437**, 509 (1985).

[11] P. Hoodbhoy and R. L. Jaffe, Phys. Rev. D **35**, 113 (1987).

[12] R. G. Arnold, P. E. Bosted, C. C. Chang, J. Gomez, A. T. Katramatou, G. G. Petratos, A. A. Rahbar, S. E. Rock, A. F. Sill, Z. M. Szalata, A. Bodek, N. Giokaris, D. J. Sherden, B. A. Mecking, and R. M. Lombard, Phys. Rev. Lett. **52**, 727 (1984).

[13] M. Arneodo *et al.*, Nucl. Phys. B **483**, 3 (1997).

[14] K. Ackerstaff *et al.*, Phys. Lett. B **475**, 386 (2000).

[15] I. R. Afnan *et al.*, Phys. Lett. B **493**, 36 (2000); G. G. Petratos *et al.*, in *Proceedings of International Workshop on the Nucleon Structure in High x-Bjorken Region (HiX2000)*, Temple University, Philadelphia, PA, USA, 2000 (url: http://inspirehep.net/record/535410?ln=en or https://arxiv.org/abs/nucl-ex/0010011); W. Melnitchouk, in *Proceedings of Workshop on the Experiments with Tritium at JLAB*, Jefferson Lab, Newport News, Virginia, 1999 (unpublished); G. G. Petratos *et al.*, in *Proceedings of Workshop on the Experiments with Tritium at JLAB*. Jefferson Lab, Newport News, Virginia, 1999 (unpublished).

[16] I. R. Afnan, F. Bissey, J. Gomez, A. T. Katramatou, S. Liuti, W. Melnitchouk, G. G. Petratos, and A. W. Thomas, Phys. Rev. C **68**, 035201 (2003); F. Bissey, A. W. Thomas, and I. R. Afnan, *ibid.* **64**, 024004 (2001).

[17] D. W. Duke and J. F. Owens, Phys. Rev. D **30**, 49 (1984).

[18] P. Hoodbhoy, Nucl. Phys. A **465**, 637 (1987).

[19] M. Modarres, J. Phys. G: Nucl. Part. Phys. **20**, 1423 (1994).

[20] M. Modarres and K. Ghafoori-Tabrizi, J. Phys. G: Nucl. Part. Phys. **14**, 1479 (1988).

[21] M. M. Yazdanpanah and M. Modarres, Phys. Rev. C **57**, 525 (1998).

[22] M. Modarres and F. Zolfagharpour, Nucl. Phys. A **765**, 112 (2006).

[23] E. Ebrahimi, M. Modarres, and M. M. Yazdanpanah, Few-Body Syst. **39**, 177 (2006); M. M. Yazdanpanah and M. Modarres, *ibid.* **37**, 33 (2005); Eur. Phys. J. A **6**, 91 (1999); **7**, 573 (2000).

[24] M. Modarres, M. M. Yazdanpanah, and F. Zolfagharpour, Eur. Phys. J. A **28**, 205 (2006).

[25] M. Modarres, M. M. Yazdanpanah, and F. Zolfagharpour, Eur. Phys. J. A **32**, 327 (2007).

[26] M. Modarres and M. Rasti, Int. J. Mod. Phys. E **22**, 1350037 (2013).

[27] M. Modarres and A. Hadian, Int. J. Mod. Phys. E **24**, 1550037 (2015).

[28] H. Nematollahi and M. M. Yazdanpanah, J. Phys. G: Nucl. Part. Phys. **44**, 075005 (2017).

[29] H. Nematollahi and M. M. Yazdanpanah, Eur. Phys. J. A **53**, 222 (2017).

[30] M. Modarres and A. Hadian, Phys. Rev. D **98**, 076001 (2018).

[31] E. G. de Oliveira, A. D. Martin, F. S. Navarra, and M. G. Ryskin, J. High Energy Phys. 09 (2013) 158.

[32] B. Lampe and E. Reya, Phys. Rep. **332**, 1 (2000).

[33] L. Frankfurt, V. Guzey, and M. Strikman, Phys. Rep. **512**, 255 (2012).

[34] L. Frankfurt and M. Strikman, Int. J. Mod. Phys. E **21**, 1230002 (2012).

[35] G. Altarelli, N. Cabibbo, L. Maiani, and R. Petronzio, Nucl. Phys. B **69**, 531 (1974).

[36] J. D. Sullivan, Phys. Rev. D **5**, 1732 (1972).

[37] A. Manohar and H. Georgi, Nucl. Phys. B **234**, 189 (1984).

[38] E. J. Eichten, I. Hinchliffe, and C. Quigg, Phys. Rev. D **45**, 2269 (1992).

[39] A. Szczurek, A. Buchmanann, and Faesller, J. Phys. G: Nucl. Part. Phys. **22**, 1741 (1996).

[40] H. Holtmann, A. Szczurek, and J. Speth, Nucl. Phys. A **596**, 631 (1996).

[41] R. C. Hwa and M. S. Zahir, Phys. Rev. D **23**, 2539 (1981).
[42] F. Arash and A. N. Khorramian, Phys. Rev. C **67**, 045201 (2003).
[43] W. Weise, *Quarks and Nuclei* (World Scientific, Singapore, 1984).
[44] M. Lavella and D. McMullan, Phys. Rep. **279**, 1 (1997).
[45] M. Traini, V. Vento, A. Mair, and A. Zambarada, Nucl. Phys. A **614**, 472 (1997).
[46] S. Scopetta, V. Vento, and M. Traini, Phys. Lett. B **421**, 64 (1998).
[47] S. Scopetta and V. Vento, Phys. Lett. B **424**, 25 (1998).
[48] S. Scopetta and V. Vento, Phys. Lett. B **460**, 8 (1999).
[49] T. Kanki, Prog. Theor. Phys. **56**, 1885 (1976).
[50] T. Kanki, Prog. Theor. Phys. **57**, 1641 (1977).
[51] H. Satz, Nuovo Cimento A **37**, 141 (1977).
[52] H. Senjo, Prog. Theor. Phys. **58**, 1651 (1977).
[53] H. Senjo, Prog. Theor. Phys. **59**, 868 (1978).
[54] S. Scopetta, V. Vento, and M. Traini, Phys. Lett. B **442**, 28 (1998).
[55] G. Altarelli, S. Petrarca, and F. Rapuano, Phys. Lett. B **373**, 200 (1996).
[56] M. M. Yazdanpanah, M. Modarres, and M. Rasti, Few-Body Syst. **48**, 19 (2010).
[57] M. Modarres and M. Rasti and M. M. Yazdanpanah, Few-Body Syst. **55**, 85 (2014).
[58] M. Modarres and A. Hadian, Nucl. Phys. A **966**, 342 (2017).
[59] S. Scopetta and V. Vento, Phys. Rev. D **71**, 014014 (2005).
[60] M. Rinaldi and S. Scopetta, Phys. Rev. C **87**, 035208 (2013).
[61] L. P. Kaptari, A. Del Dotto, E. Pace, G. Salmé, and S. Scopetta, Phys. Rev. C **89**, 035206 (2014).
[62] S. Fucini, S. Scopetta, and M. Viviani, Phys. Rev. C **98**, 015203 (2018).
[63] M. Glück, P. Reya, and A. Vogt, Z. Phys. C **67**, 433 (1995).
[64] B. E. Matthias, H. E. Ahn, A. Badertscher, F. Chmely, M. Eckhause, V. W. Hughes, K. P. Jungmann, J. R. Kane, S. H. Kettell, Y. Kuang, H.-J. Mundinger, B. Ni, H. Orth, G. zu Putlitz, H. R. Schaefer, M. T. Witkowski, and K. A. Woodle, Phys. Rev. Lett. **66**, 2716 (1991).
[65] M. Arneodo *et al.*, Phys. Rev. D **50**, R1 (1991).
[66] A. De Rujula and F. Martin, Phys. Rev. D **22**, 1787 (1980).
[67] P. Gonzalez *et al.*, Z. Phys. A **350**, 371 (1995).
[68] C. Ciofi degli Atti and S. Liutu, Phys. Rev. C **41**, 1100 (1990).
[69] A. Del Dotto, E. Pace, G. Salmé, and S. Scopetta, Phys. Rev. C **95**, 014001 (2017).
[70] R. C. Barrett and D. F. Jackson, *Nuclear Sizes and Structure* (Clarendon, Oxford, 1997).
[71] G. G. Petratos, J. Gomez, R. J. Holt, and R. D. Ransome (MARATHON Collaboration), Jefferson Lab Experiment, Proposal No. C12-10-103 (2010).
[72] N. Isgur and G. Karl, Phys. Rev. D **18**, 4187 (1978).
[73] N. Isgur and G. Karl, Phys. Rev. D **19**, 2653 (1979).
[74] N. Isgur and G. Karl, Phys. Rev. D **23**, 817 (1981).
[75] R. Bijker, F. Iachello, and A. Leviatan, Ann. Phys. **236**, 69 (1994).
[76] R. Bijker, F. Iachello, and A. Leviatan, Phys. Rev. C **54**, 1935 (1996).
[77] R. Bijker, F. Iachello, and A. Leviatan, Phys. Rev. D **55**, 2862 (1997).
[78] P. Amaudruz *et al.*, Nucl. Phys. B **441**, 3 (1995).
[79] L. W. Whitlow *et al.*, Phys. Lett. B **282**, 475 (1992).
[80] W. Melnitchouk and A. W. Thomas, Phys. Lett. B **377**, 11 (1996).
[81] A. Bodek, M. Breidenbach, D. L. Dubin, J. E. Elias, J. I. Friedman, H. W. Kendall, J. S. Poucher, E. M. Riordan, M. R. Sogard, D. H. Coward, and D. J. Sherden, Phys. Rev. D **20**, 1471 (1979).
[82] M. R. Adams *et al.*, Phys. Rev. Lett. **75**, 1466 (1995).